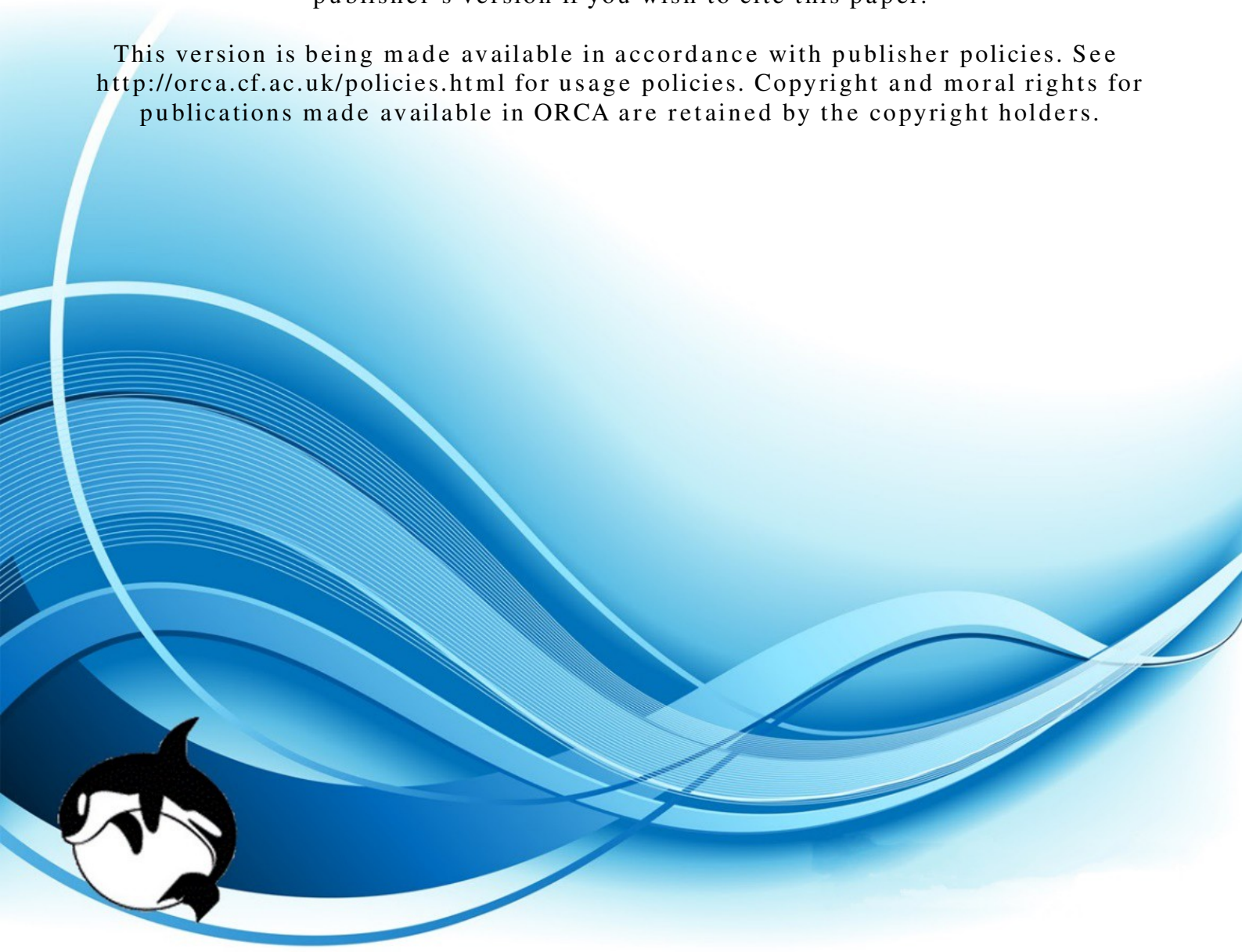

Pure and Applied Geophysics

Scaling laws for the distribution of some natural resources

--Manuscript Draft--

Manuscript Number:	
Full Title:	Scaling laws for the distribution of some natural resources
Article Type:	Report-Top.Vol. Fractals and Dynamic Systems in Geoscience
Keywords:	Mass dimension; fractal; resource; gold; percolation; unconventional gas resource
Corresponding Author:	Thomas Blenkinsop Cardiff University Cardiff, UNITED KINGDOM
Corresponding Author Secondary Information:	
Corresponding Author's Institution:	Cardiff University
Corresponding Author's Secondary Institution:	
First Author:	Thomas Blenkinsop
First Author Secondary Information:	
Order of Authors:	Thomas Blenkinsop
Order of Authors Secondary Information:	
Abstract:	Mass dimensions of natural resources, established from power law scaling relationships between numbers of resources and distance from an origin, have important implications for ore-forming processes, resource estimation and exploration. The relation between the total quantity of resource and distance, measured by the mass-radius scaling exponent, may be even more useful. Lode gold deposits, geothermal wells and volcanoes, and conventional and unconventional gas wells are examined in this study. The scaling exponents generally increase from the lode gold through geothermal wells to gas data sets, reflecting decreasing degrees of clustering. Mass dimensions are similar to the mass-radius scaling exponents, and could be used as substitutes in the common case that data are not available for the latter. All of these resources are formed by fluid fluxes in the crust, and therefore percolation theory is an appropriate unifying framework to understand their significance. The mass dimensions indicate that none of the percolation networks that formed the deposits reached the percolation threshold.
Suggested Reviewers:	Dave Sanderson D.J.Sanderson@soton.ac.uk Expert on fractals and Natural Resources
	Pablo Gumiel Pablo.gumiel@uah.es Expert of fractals and Natural Resources
	Jon Hronsky jon.hronsky@wesminllc.com Expert on mineral deposits, exploration and resource estimation
	Julian Vearncombe julian@sjsresource.com.au Expert on gold and other mineral deposits
	Steve Cox Stephen.Cox@anu.edu.au First to apply the concept of percolation theory to mineral deposits

Scaling laws for the distribution of some natural resources

Tom Blenkinsop

School of Earth and Ocean Sciences

Cardiff University

Main Building, Park Place

Cardiff CF10 3AT

BlenkinsopT@Cardiff.ac.uk

Abbreviated title: **Scaling laws for natural resource distribution**

Abstract

Mass dimensions of natural resources, established from power law scaling relationships between numbers of resources and distance from an origin, have important implications for ore-forming processes, resource estimation and exploration. The relation between the total quantity of resource and distance, measured by the mass-radius scaling exponent, may be even more useful. Lode gold deposits, geothermal wells and volcanoes, and conventional and unconventional gas wells are examined in this study. The scaling exponents generally increase from the lode gold through geothermal wells to gas data sets, reflecting decreasing degrees of clustering. Mass dimensions are similar to the mass-radius scaling exponents, and could be used as substitutes in the common case that data are not available for the latter. All of these resources are formed by fluid fluxes in the crust, and therefore percolation theory is an appropriate unifying framework to understand their significance. The mass dimensions indicate that none of the percolation networks that formed the deposits reached the percolation threshold.

Key words. Mass dimension; fractal; resource; gold; percolation; unconventional gas resource

1. Introduction

Scaling laws have been applied to many aspects of natural resources. Mandelbrot (1983) suggested that mineral distribution in the Earth might be a fractal dust, and this idea has been followed up for hydrothermal mineral deposits (e.g. Carlson 1991; Blenkinsop 1994, 1995; Raines, 2008; Carranza 2009) and petroleum deposits (Barton and Scholz 1995). Fractal relations between ore grade and tonnage were described by Turcotte (1986), and fractal aspects

of structures in vein-hosted deposits have been described by Sanderson et al. (1994), Roberts et al. (1999), Johnston and McCaffrey (1996) and Nortje et al. (2006) among others. Fractal applications of geochemistry to natural resources have been well documented (e.g. Agterberg 1995; Agterberg et al. 1996; Cheng et al. 1994; Cheng 1999a, b, c, d). Describing the distribution of natural resources is useful in order to estimate total resources (e.g. Barton and Scholz 1995), and also has important implications for exploration strategies (e.g. Ford and Blenkinsop 2008), and for processes by which natural resources form (e.g. Arias et al. 2011).

The box counting method has been widely applied to quantify the distribution of natural resources, for example mineral deposits:

$$N(\delta) \sim \delta^{Db}$$

Where $N(\delta)$ is the number of boxes of side δ required to cover the deposits. *Db* is the box-counting dimension, which is a measure of clustering (e.g. Carlson 1991). Uniform or random distributions have $Db = 2$; increasing degrees of clustering have smaller values of *Db*. A more useful description of resource distribution may be given by the relation:

$$M(r) \sim r^{-Dm}$$

where $M(r)$ is the mass of resource within a circle of radius r (e.g. La Pointe, 1995). If the mass of each resource occurrence is unity, this law describes the mass dimension *Dm* of the resource. *Dm* is also simply interpreted as a measure of the clustering of the resource distribution. The mass-radius relationship is sometimes expressed as the radial density function:

$$d(r) \sim r^{-Dm-2}$$

where $d(r) = M(r)/\pi r^2$ is the density of deposits as a function of r (e.g. Raines 2008).

However, the mass of resources typically varies at each location. This can be quantified by a general scaling law:

$$M(r) \sim r^{-Dmr}$$

Dmr is referred to here as the mass-radius scaling exponent. This exponent can have values greater than 2, and is potentially a more complete description of the distribution of natural resources because it measures variations in mass of resource at each locality.

Mass dimensions have been investigated in diverse research fields, including astrophysics (e.g. Duval et al. 2010), neurobiology (e.g. Caserta et al. 1995), particle science (Liao et al. 2005), and texture analysis (e.g. Backes and Bruno 2013), but they have not been widely applied to natural resources. Box counting and mass dimensions have been determined for gold deposits (e.g. Carlson 1991; Blenkinsop 1994, 1995, Carranza 2009; Carranza et al. 2009; Carranza 2010; Carranza and Saghedi 2010) and for petroleum deposits (Barton and Scholz 1995), but mass-radius scaling exponents are hardly reported in the literature. The aim of this paper is to investigate mass dimensions and the suitability of the mass-radius scaling exponent to describe the distribution of some natural resources. Hydrothermal gold deposits, geothermal wells and volcanic vents, and gas wells are considered in this study. Each of the data sets represents the product of fluid flow systems in the crust; hence the relevance of percolation theory to the results is also considered.

2. *Data and Methods*

Mass dimensions and mass-radius scaling exponents have been determined in this study for Archean gold deposits in Zimbabwe (Figs. 1, 2), divided into a data set for the whole craton and a more detailed data set from the Masvingo area. Geothermal wells and volcanoes in Oregon (Fig. 3), and conventional and unconventional gas production in Pennsylvania (Figs. 4, 5, 6) were also analysed. Details of the data and sources are given in Table 1. In the Pennsylvania data, unconventional wells are considered as those drilled "for the purpose of or to be used for the production of natural gas from an unconventional formation" (https://www.paoilandgasreporting.state.pa.us/publicreports/Modules/DataExports/DataExports.aspx). All conventional wells are vertical, but most unconventional wells are horizontal. Virtually all unconventional wells, and by far the majority of conventional wells, produced gas only; there was some oil production from a few conventional wells.

Figs 1 – 6 here

Expanding circles used to count mass around a point were entirely constrained within the study area limits to avoid edge effects, and "mass" was normalized to the total value of the data sets ΣM, so that $M'(r) = M(r)/ \Sigma M$. Two strategies were investigated for determining the exponents of the scaling laws:

1) A grid origin method, in which the mass was summed and averaged from expanding circles centred on 100 origins on grid nodes in the central part of the study area (cf. La Pointe 1995).
2) A data point origin method, in which counting circles were centred on data points, and average values were taken from every circle used.

Both methods were applied to the coordinates of the Koch curve as well as to all data sets. The grid origin method produced exponents with values that were all near 2, including for the Koch curve, and showed little variation between data sets. By contrast, the data point origin method returned a value of 1.26 for the Koch curve (the curve has a fractal dimension of 1.26; e.g. Peitgen et al. 2004), and discriminated sensitively between the data sets. Hence it was used for all results shown in this study.

Mass dimensions could be calculated for all data sets, and mass-radius scaling exponents could be calculated for gold production from the Zimbabwe craton and gas production from Pennsylvania, because these data sets included resource figures. Exponents were obtained by regression of log *M'(r)* against log *r* over the linear part of the scaling relationship, for a range of *r* of 1 to 1.5 orders of magnitude. Lower and upper limits of regression are shown in Table 1.

3. Results

Linear parts of all data sets can be defined over at least an order of magnitude (Figs. 7 - 10), justifying the above regression technique. The data sets showed two characteristic features. At both low and high values of *r*, the slopes of the log mass-radius relations were less than the central part of the data, where the regression was carried out (e.g. Fig. 7). Mass dimensions vary between 1.2 and 1.8 (Table 2). Standard errors of regression vary from 0.009 to 0.017, indicating that the range of mass dimensions measured shows significantly different degrees of clustering between different data sets.

Figs. 7 – 10 here

The gold deposits of the Zimbabwe craton have the lowest mass dimensions of all data sets

considered, indicating the greatest degrees of clustering (Table 2). The mass-radius scaling exponent is within regression error of the mass dimension for the cratonic data set. The mass dimension for the Masvingo data set is significantly greater than for the craton data.

The geothermal wells of Oregon have a stepped log mass-radius relation (Fig. 8) in which two segments of similar slope are offset from one another. The mass dimension of the larger part of the data is 1.23 (Table 2). The volcanic vents of Orgeon have a mass dimension of 1.51 (Fig. 8).

Unconventional gas wells in Pennsylvania have mass dimensions of 1.26 (producing wells) and 1.45 (all wells) (Table 2). The mass-radius scaling exponent of the producing wells, 1.32, lies between these values. The highest values of mass dimension are from conventional gas production, (1.57 and 1.63 for all wells and producing wells respectively). The mass-radius exponent of the producing wells is the highest value measured, 1.72.

4. Discussion

4.1 Consistency with previous results

Mass dimensions of various types of gold deposit have been presented by Blenkinsop (1994, 1995), Carranza (2009; 2010) and Carranza et al. (2009). In all these studies, different fractal dimensions are given at low and high r values, ranging from 0.54 for the low r values, to 1.52 (high r). Mass-radius scaling exponents were calculated for nine hydrocarbon plays by La Pointe (1995) using area of hydrocarbon fields as a measure of mass, and reported as between 1 and 2. The mass dimensions and mass-radius scaling exponent reported here are therefore broadly consistent with the few previous results reported in the literature from similar commodities.

4.2 Non-linearity of logarithmic mass-radius scaling

The log mass-radius scaling relations examined are characteristically non-linear at values of r generally less than 1000 m, illustrated for the Masvingo data set in Fig. 7, but also seen at lower values of r than shown in the other data sets. This non-linearity is similar to the "roll-off" observed in box-counting plots at low δ values (e.g. Pickering et al. 1995). For gold deposits of the Zimbabwe craton, this effect this effect has been attributed to random sampling of a fractal data set (Blenkinsop and Sanderson 1999), and it seems likely that the same explanation applies here, i.e. that the actual data sets represent samples of a true fractal distribution. The log mass-radius relations show less mass at high values of r than predicted by a linear relation. It is noticeable that the non-linearity occurs at radii that are about ¼ of the maximum linear dimension of the study areas or greater. Counting circles with these large r values are only taken from the centre of the study areas: thus, concentrations of resources near the corners will not be included, possibly leading to a deficit, in the case of clustering near the peripheries of the study areas.

4.3 Mass dimensions of data sets vs. natural resources

True mass dimensions of natural resources should reflect resource-forming process. For hydrothermal mineral deposits and hydrocarbons, this may include elements of source distribution, fluid transport and deposition (trapping mechanisms). However, mass dimensions estimated from resource databases such as those used here will be influenced by the degree of exploration and other economic factors. The extent to which the Zimbabwe data are affected by this is discussed in Blenkinsop and Sanderson (1999), but how well the other data sets used here reflect the actual distribution of resources in the Earth is unknown. The production of gas from horizontal drilling (e.g. Arthur et al. 2008) could affect the distribution of wells on a hundred m scale.

Despite the possible influence of non-geological factors, the results reported here make geological sense. Hydrothermal mineral deposits such as gold are strongly structurally controlled by specific deformation zones (e.g. Groves et al. 1998; Wit and Vanderhor 1998; Cox 1999). This leads to strong clustering of gold deposits (Blenkinsop 1994, 1995, Caranza 2009). Hydrocarbon resources, including gas, are also structurally controlled: the influence of structure in the Marcellus Shale can clearly be seen at a small scale (Fig. 6). Source and trap rock types and burial history are also very important, and the generally low values of mass dimensions for the gas resources of Pennsylvania reflect the presence of the Marcellus Shale under most of the state. Shale gas is formed and trapped in situ in shales, so that the host rock is both source and reservoir, and thus potentially making large parts of the Marcellus shale that have had the correct burial history into unconventional gas sources (Kargbo et al. 2010), and giving a less clustered distribution than the gold deposits.

The distribution of geothermal wells is related to geothermal structure, which is a function of tectonics. The tectonics of Oregon are dominated by the Cascadia subduction zone, which creates the Cascade volcanic arc and determines the location of volcanoes (Priest 1990). Heat flow is thought to be influenced by the presence of partial melts in the mid crust at depths of 10 km (Blackwell et al. 1990). However, on a more local scale in North-Central Oregon, regional groundwater flow modifies the conductive flux by sweeping heat from young elevated rocks into adjacent older rocks at lower elevations (Ingebritsen et al. 1989; Blackwell et al. 1990).

4.4 Percolation theory: a unifying framework

The formation of all the georesources considered above is linked by fluid flow. A possible unifying framework for considering the mass dimensions and mass-radius scaling exponents is therefore percolation theory. This concept has been applied to the formation of hydrothermal gold

deposits (Cox 1999) in the context of fluid flow in fracture networks (e.g. Rivier et al. 1985), and there is an extensive literature on applications of percolation theory to primary migration of hydrocarbons (e.g. Carruthers and Ringrosem 1998; Carruthers 2003; Corradi et al. 2009). General aspects of percolation theory may therefore assist with interpretation of the results presented here (cf. Cox 1999).

A percolation network consists of a lattice in which some sites are occupied, with a probability p of occupation (Stauffer and Aharony 1994). As the network evolves, p changes. Many aspects of percolation networks are fractal, for example the dimensions and numbers of clusters of occupied sites, and times for their evolution. As p increases, a critical stage is reached called the percolation threshold, defined as the point at which a continuous path of occupied nodes exists from one side of the network to the other, and the network changes from closed to open. The percolation threshold occurs at a critical probability pc. Fractal dimensions of percolation networks change over a considerable range as p increases, but can be simplified into three conditions: $p < pc$, $p = pc$ and $p > pc$. Two and three dimensional mass dimensions for percolation networks consisting of a Bethe lattice (in which every site has the same number of neighbours and there are no closed loops) in these three stages are shown in Table 3.

The study areas of the Zimbabwe craton, Oregon, and Pennsylvania, have linear dimensions of hundreds of km compared to crustal thicknesses of tens of km (Nelson, 1992; Nguuri et al. 2000; Eagar et al. 2011). It may therefore be reasonable to compare the mass dimensions of this study to those of 2D percolation networks. All the mass dimensions measured here are below the mass dimensions of 2D Bethe lattices at the percolation threshold. In the case of gold deposits, this is intuitively reasonable. Once a backbone, network-spanning cluster has formed in a hydrothermal system, the localization of fluid flow along this structure would preclude mineralization

elsewhere. Mass dimensions of the gas wells are closer to the 2D threshold value, which may be reflected in their more distributed pattern (Fig. 9). It is also reasonable that the gas has not attained a percolation threshold for the same reason as the gold deposits: once a percolation threshold is reached, the reservoir would be breached and no resources would remain.

4.5 The relation between mass dimension and mass-radius scaling exponent

Mass dimensions and mass-radius scaling exponents have obvious applicability to resource estimation (e.g. Barton and Scholz 1995; La Pointe, 1995). However, it is commonly hard to measure the mass-radius scaling exponent because accurate data for "mass" (resources) is difficult to obtain. The mass dimensions and mass-radius scaling exponents are similar for the three data sets in which they could be compared. If this relationship was generally true, an approximate value for the mass-radius scaling exponent can be given by the mass dimension.

5. Conclusions

Mass dimensions of hydrothermal gold deposits, volcanic vents, geothermal wells and gas wells can be determined reliably from appropriate databases. How accurately these values reflect the true distribution of natural resources is not known, but the low mass dimensions of hydrothermal gold deposits compared to gas wells is consistent with a high degree of localization of the gold deposits due to strong structural controls, compared to a relatively dispersed pattern of gas accumulations, for which the widespread presence of the Marcellus shale as a source and a host is one of the most important factors in determining their distribution. Mass dimensions of volcanic vents and geothermal wells are intermediate between the gold and gas values. The mass-radius scaling exponent (i.e. the variation of mass with distance including a measure of the resource) was

estimated for gold and gas data sets. This exponent is similar to the mass dimension; the latter could be used as a proxy for the mass-radius scaling exponent where resource estimates are not available. Percolation theory offers a framework for understanding the significance of the mass dimension and mass-radius exponents: the percolation threshold may not have been reached for the resources considered here.

Acknowledgements

Diego Perugini and the staff at the Universita degli Studi di Perugia are gratefully acknowledged for organizing the 6th International Conference on Fractals and Dynamic systems in Geosciences. Ian Merrick assisted with programming in C++.

REFERENCES

Agterberg F.P. (1995), Multifractal modeling of the sizes and grades of giant and supergiant deposits, Int. Geol. Rev. 37, 1–8.

Agterberg, F.P., Cheng Q., and Wright, D.F. (1996) Fractal Modelling of Mineral Deposits, In (eds) Proceedings of the International Symposium on the Application of Computers and Operations Research in the Minerals Industries (ed. Elbrond J, Tang X.) (Montreal) pp 43– 53.

Arias, M., Gumiel, P., Sanderson, D.J., and Martin-Izard,A. (2011), A multifractal simulation model for the distribution of VMS deposits in the Spanish segment of the Iberian Pyrite Belt, Comp. & Geosciences, 37, 1917-1927, doi: 10.1016/j.cageo.2011.07.012.

Arthur, J. D., and Bohm, B., Mark Layne, M. (2008), Hydraulic fracturing considerations for natural gas wells of the Marcellus Shale, Groundwater Protection Council Annual Forum. Cincinnati. 2008.

Backes, A.R., and Bruno, O.M. (2013), Texture analysis using volume-radius fractal dimension, App. Math. Computation 219, 5870–5875.

Bartholomew, D. S. 1990. Gold Deposits in Zimbabwe. Geological Survey of Zimbabwe Mineral Resources Series, 23.

Barton, C.C. and Scholz, C.H. (1995), The fractal size and spatial distribution of hydrocarbon accumulations; implications for resource assessment and exploration strategy, In Fractals in petroleum geology and earth processes (ed. Barton, C.C. and La Pointe, P.R.) (Plenum Press, New York and London 1995), pp. 13-34.

Blackwell, D.D., Steele, J.L., Frohme, M.K., Murphey, C.F., Priest, G.R., and Black, G. L. (1990), Heat Flow in the Oregon Cascade Range and its Correlation with regional gravity, Curie Point depths, and geology. J. Geophys. Res. 95, B12, 19475-19493.

Blenkinsop, T. (1994), The Fractal Distribution of Gold Deposits: two examples from the Zimbabwe Archaean craton, in Fractals and Dynamic Systems in Geoscience (ed. Kruhl, J.) (Springer-Verlag) pp. 247–258.

Blenkinsop, T. (1995), Fractal measures for size and spatial distributions of gold mines: economic applications, In Sub-Saharan Economic Geology (ed. Blenkinsop, T.G., Tromp, P.) (A.A. Balkema, Rotterdam) pp. 177–186.

Blenkinsop, T.G., and Sanderson, D.J. (1999), Are gold deposits in the crust fractals? A study of gold mines in the Zimbabwe craton, Geol. Soc. London, Spec. Publ. 155, 141–151.

Carlson, C.A. (1991), Spatial distribution of ore deposits, Geology 19, 111–114

Carranza, E.J.M., Hale, M., and Mangaoang, J.C. (1999), Application of mineral exploration models and GIS to generate mineral potential maps as input for optimum land-use planning in the Philippines, Nat. Res. Research 8, 165–173.

Carranza, E.J.M. (2009), Controls on mineral deposit occurrence inferred from analysis of their spatial pattern and spatial association with geological features, Ore Geology Reviews 35, 383-400.

Carranza, E.J.M., Owusu, E.A., and Hale, M. (2009), Mapping of prospectivity and estimation of number of undiscovered prospects for lode gold, southwestern Ashanti Belt, Ghana, Min. Deposita 44, 915-938.

Carranza, E. J. M. (2010), From Predictive Mapping of Mineral Prospectivity to Quantitative Estimation of Number of Undiscovered Prospects, Resource Geology 61. 30 – 51. DO - 10.1111/j.1751-3928.2010.00146.x

Carranza, E.J.M., and Sadeghi, M. (2010), Predictive mapping of prospectivity and quantitative estimation of undiscovered VMS deposits in Skellefte district (Sweden), Ore Geol. Reviews 38, 219-241.

Carruthers, D.J. (2003), Modelling of secondary petroleum migration using invasion percolation techniques, in: (Eds.), Multidimensional basin modeling, AAPG Discovery Series, (eds. Duppenbecker, S., Marzi, R.) (AAPG 2003) vol. 7, chapter 3.

Carruthers, D., and Ringrosem, P. (1998), Secondary oil migration: oil-rock contact volumes, flow behaviour and rates, Geological Society London Special Publications, 144, 205–220.

Caserta, F., Eldred, W.D., Fernandez, E., Hausan, R.E., Stanford, L.R., Bulderev, S.V., Schwarzer, S., and Stanley, H.E. (1995), Determination of fractal dimension of physiologically characterized neurons in two and three dimensions. J. Neuroscience Methods 56, 133-144.

Cheng, Q. (1999a), The gliding box method for multifractal modeling, Comput. Geosci. 25, 1073–1079.

Cheng, Q. (1999b), Markov processes and discrete multifractals, Math. Geol. 31, 455–469.

Cheng, Q. (1999c), Multifractality and spatial statistics, Comput. Geosci. 25, 949–961.

Cheng, Q. (1999d), Spatial and scaling modelling for geochemical anomaly separation, J Geochem Explor 65, 175–194.

Cheng Q., Agterberg F.P., and Ballantyne S.B. (1994), The separation of geochemical anomalies from background by fractal methods, J. Geochem Explor. 51, 109–130.

Corradi, A., Ruffo, P., Corrao, A., Visentin, C. (2009), 3D hydrocarbon migration by percolation technique in an alternate sand–shale environment described by a seismic facies classified volume. Marine and Petroleum Geology 26, 495-503.

Cox, S.F. (1999), Deformational controls on the dynamics of fluid flow in mesothermal gold systems, Geological Society London Special Publications 155, 123–140.

Duval, J., Jackson, J.M., Heyer, M., Rathbone, J., and Simon, R. (2010), Physical Properties And Galactic Distribution Of Molecular Clouds Identified In The Galactic Ring Survey, Astrophys. Journal, 723, 492–507.

Eagar, K. C., Fouch, M. J., James, D.E. and Carlson, R.W. (2011), Crustal structure beneath the High Lava Plains of eastern Oregon and surrounding regions from receiver function analysis, J. Geophys. Res., 116, B02313, doi:10.1029/2010JB007795.

Ford, A., and Blenkinsop, T.G. (2008), Combining fractal analysis of mineral deposit clustering with weights of evidence to evaluate patterns of mineralization: Application to copper deposits of the Mount Isa Inlier, NW Queensland, Australia, Ore Geol. Rev. 33, 435–450.

Groves, D.I., Goldfarb, R.J., Gebre-Mariam, M., Hagemann, S.G., and Robert, F. (1998), Orogenic gold deposits: A proposed classification in the context of their crustal distribution and relationship to other gold deposit types, Ore Geol. Rev. 13, 7–27.

Ingebritsen, S. E., Sherrod, D.R., and Mariner, R.H. (1989), Heat Flow and Hydrothermal Circulation in the Cascade Range, North-Central Oregon, Science 243, 1458-1462.

Johnston, J.D., and McCaffrey, K.J.W. (1996), Fractal geometries of vein systems and the variation of scaling relationships with mechanism, J. Struc. Geol. 18, 349–358.

Kargbo, D.M., Wilhelm, R.G., and Campbell, D.J. (2010), Natural gas plays in the Marcellus Shale: challenges and potential opportunities, Environ. Sci. Technol. 44, 5679–84.

La Pointe, P.R. (1995), Estimation of Undiscovered Hydrocarbon Potential through Fractal Geometry, In Fractals in petroleum geology and earth processes (ed. Barton, C.C. and La Pointe, P.R.) (Plenum Press, New York and London 1995), pp. 35-57.

Liao, J.Y.H. Selomulya, C., Bushell, G., Bickert, G., and Amal, R. (2005), On different approaches to estimate the mass fractal dimension of coal aggregates, Part. Part. Syst. Charact. 22, 299–309. DOI: 10.1002/ppsc.200500978

Mandelbrot, B.B., The Fractal Geometry of Nature, (W.H. Freeman and Company, New York 1983).

Nelson, K.D. (1992), Are crustal thickness variations in old mountain belts like the Appalachians a consequence of lithospheric delamination? Geology, 20, 498-502. doi: 10.1130/0091-7613(1992)020<0498:ACTVIO>2.3.CO;2

Nguuri, T. K., Gore, J., James, D. E., Webb, S. J., Wright, C., Zengeni, T. G., Gwavava, O., and Snoke, J. A. (2000), Crustal structure beneath southern Africa and its implications for the formation and evolution of the Kaapvaal and Zimbabwe cratons, Geophys. Res. Letters, 28, 2501-2504. 10.1029/2000GL012587

Nortje, G.S., Rowland, J.V., Spörli, K.B., Blenkinsop, T.G., and Rabone, S.D.C. (2006), Vein deflections and thickness variations of epithermal quartz veins as indicators of fracture coalescence, J. Struct. Geol. 28, 1396–1405.

Peitgen, H-O, Jurgens, H., and Saupe, D. (2004), Chaos and Fractals: New Frontiers of Science, (Springer 2004).

Pickering, G., Bull, J. M., and Sanderson, D. J. (1995), Sampling Power-Law distributions.

Tectonophys, 248, 1-20.

Priest, G. R. (1990), Volcanic and tectonic evolution of the Cascade Volcanic Arc, central Oregon, J. Geophys. Res., 95(B12), 19583–19599, doi:10.1029/JB095iB12p19583.

Raines, G. L. (2008), Are fractal dimensions of the spatial distribution of mineral deposits meaningful? Nat. Resour. Res., 17, 87–97.

Rivier, N., Guyon, E., and Charlaix, E. (1985), A geometrical approach to percolation through random fractured rocks, Geol. Mag. 122, 157-162.

Roberts, S., Sanderson, D.J., and Gumiel, P. (1999), Fractal analysis and percolation properties of veins, Geological Society London Special Publication 155. 7-16.

Sanderson, D.J., Roberts, S., and Gumiel, P. (1994), A Fractal Relationship between Vein Thickness and Gold Grade in Drill Core from La Codosera, Spain, Econ. Geol. 89, 168–173.

Stauffer, D., and Aharony, A., Introduction to Percolation theory, (CRC press, Florida 1994).

Turcotte D.L. (1986), A Fractal Approach to the Relationship between Ore Grade and Tonnage. Econ. Geol. 81, 1528–1532.

Wilson, J. F. (1964), The geology of the country around Fort Victoria. Bulletin of the Rhodesian Geological Survey, 58.

Wilson, J. F. (1968), The geology of the country around Mashaba. Bulletin of the Rhodesian Geological Survey, 68.

Witt, W.K., and Vanderhor, F. (1998), Diversity within a unified model for Archaean gold mineralization in the Yilgarn Craton of Western Australia: An overview of the late-orogenic, structurally-controlled gold deposits, Ore Geol. Rev. 13, 29-64.

FIGURES

Fig. 1. Gold mines in Zimbabwe, with symbols scaled by log production. From Bartholomew (1991). UTM coordinates, WGS84 Datum.

Fig. 2. Gold occurrences in the Masvingo area, Zimbabwe. From Wilson (1964, 1968). UTM coordinates, WGS84 Datum.

Fig. 3. Geothermal wells and volcanoes, Oregon County. From http://www.oregongeology.com/sub/gtilo/index.htm. UTM coordinates, NAD83 Datum.

Fig. 4. Conventional gas wells in Pennsylvania with producing well distinguished. From https://www.paoilandgasreporting.state.pa.us/publicreports/Modules/DataExports/DataExports.aspx. All Pennsylvanian maps are UTM coordinates with a WGS84 datum.

Fig. 5. Unconventional gas wells in Pennsylvania, with producing wells distinguished. Source as in Fig. 4.

Fig. 6. Detail of distribution of conventional gas wells, showing a structural control. Source as in Fig. 4.

Fig. 7. Variation of Logarithm of mass with radius (Logarithmic Mass-radius function) for Masvingo and Craton gold deposit data sets, with regression lines used shown.

Fig. 8. Logarithmic mass-radius function for Oregon data sets (volcanic vents and geothermal wells), with regression lines used shown.

Fig. 9. Logarithmic mass-radius function for Pennsylvania data sets (conventional gas production), with regression lines used shown.

Fig. 10. Mass-radius function for Pennsylvania data sets (unconventional gas production), with regression lines used shown.

Figure1
Click here to download high resolution image

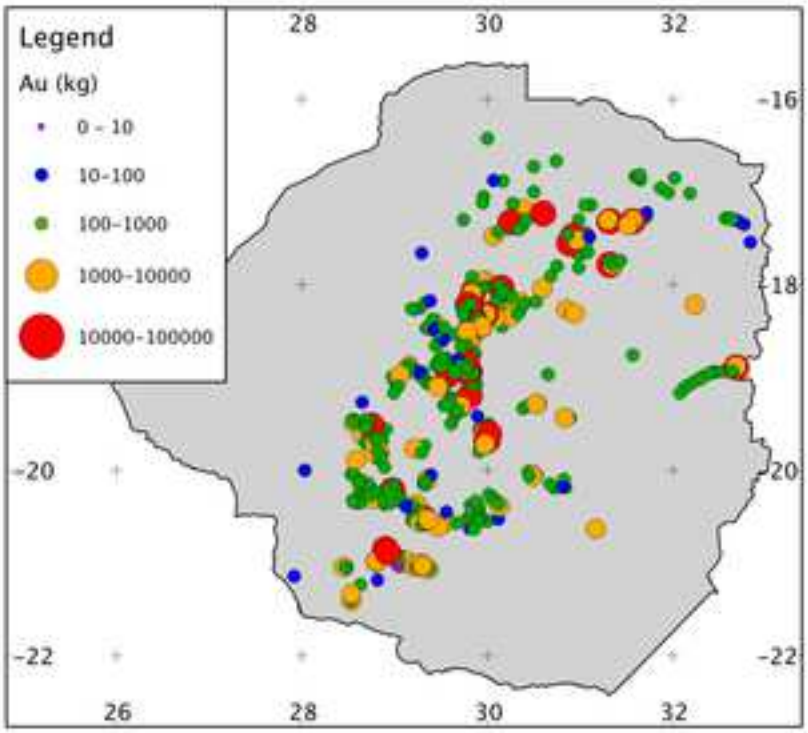

Figure2
Click here to download high resolution image

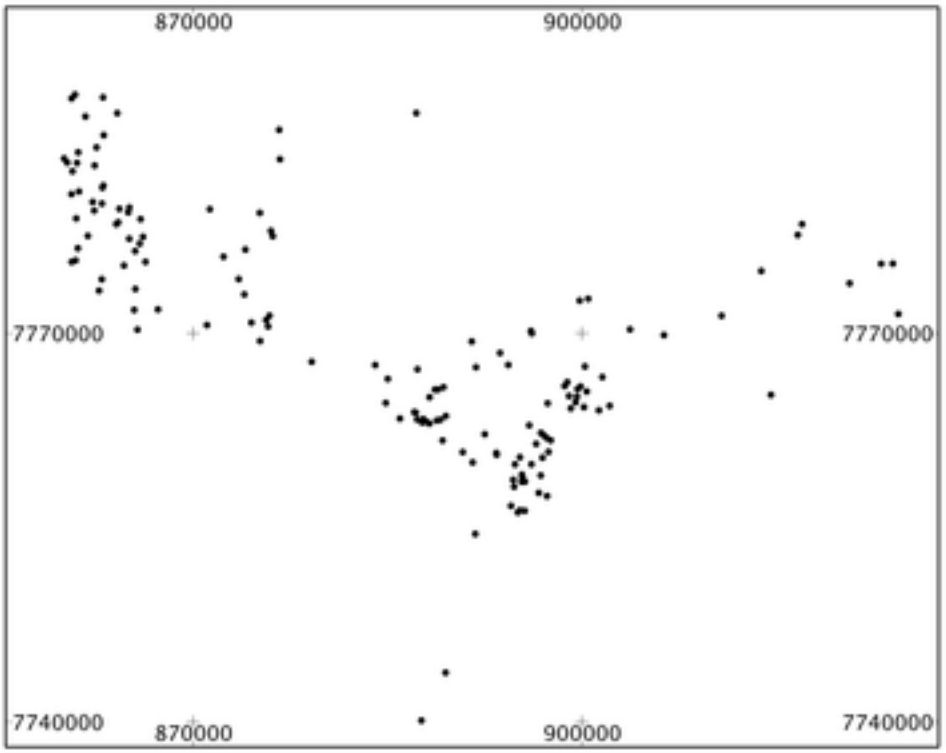

Figure3
Click here to download high resolution image

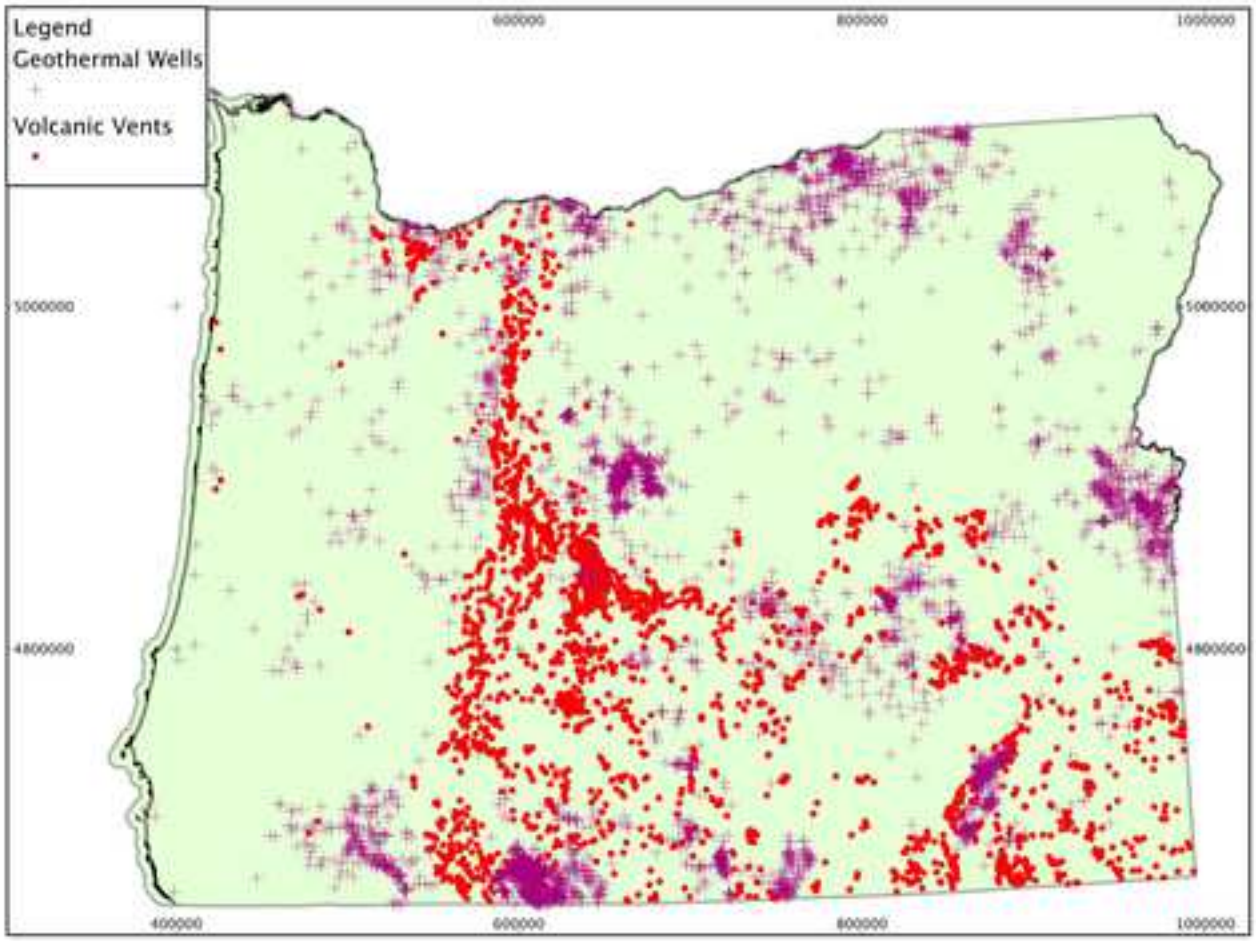

Figure4
Click here to download high resolution image

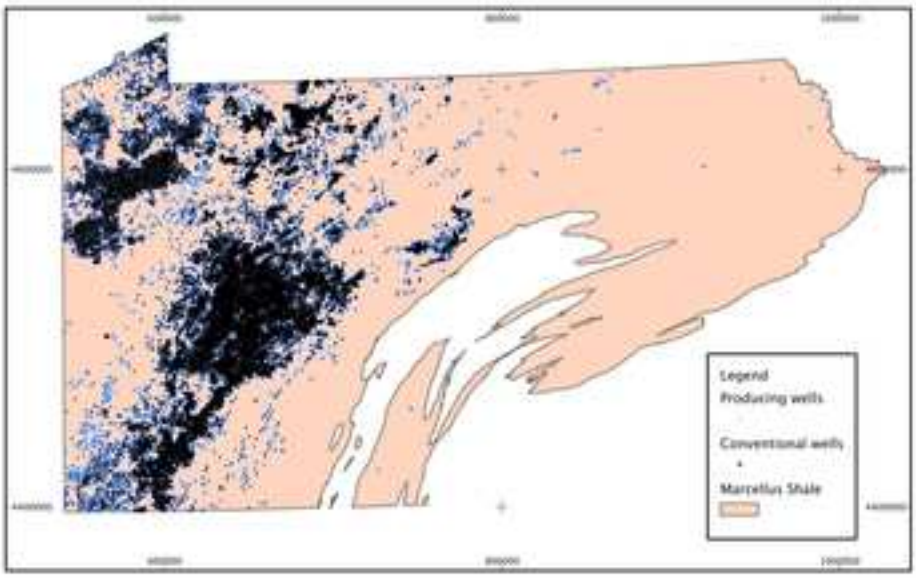

Figure5

Click here to download high resolution image

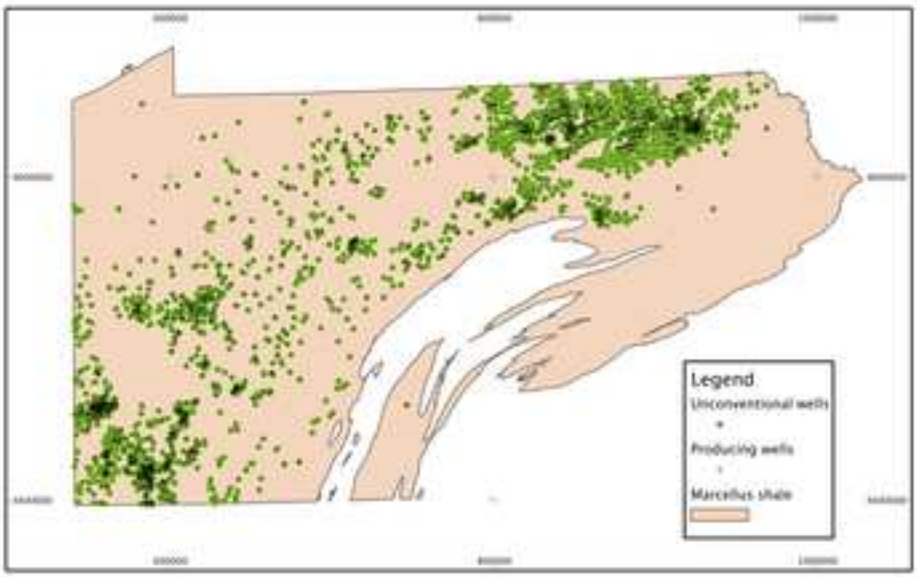

Figure6
Click here to download high resolution image

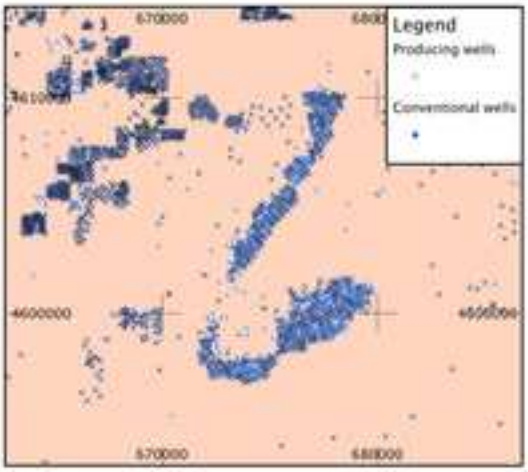

Figure7
Click here to download high resolution image

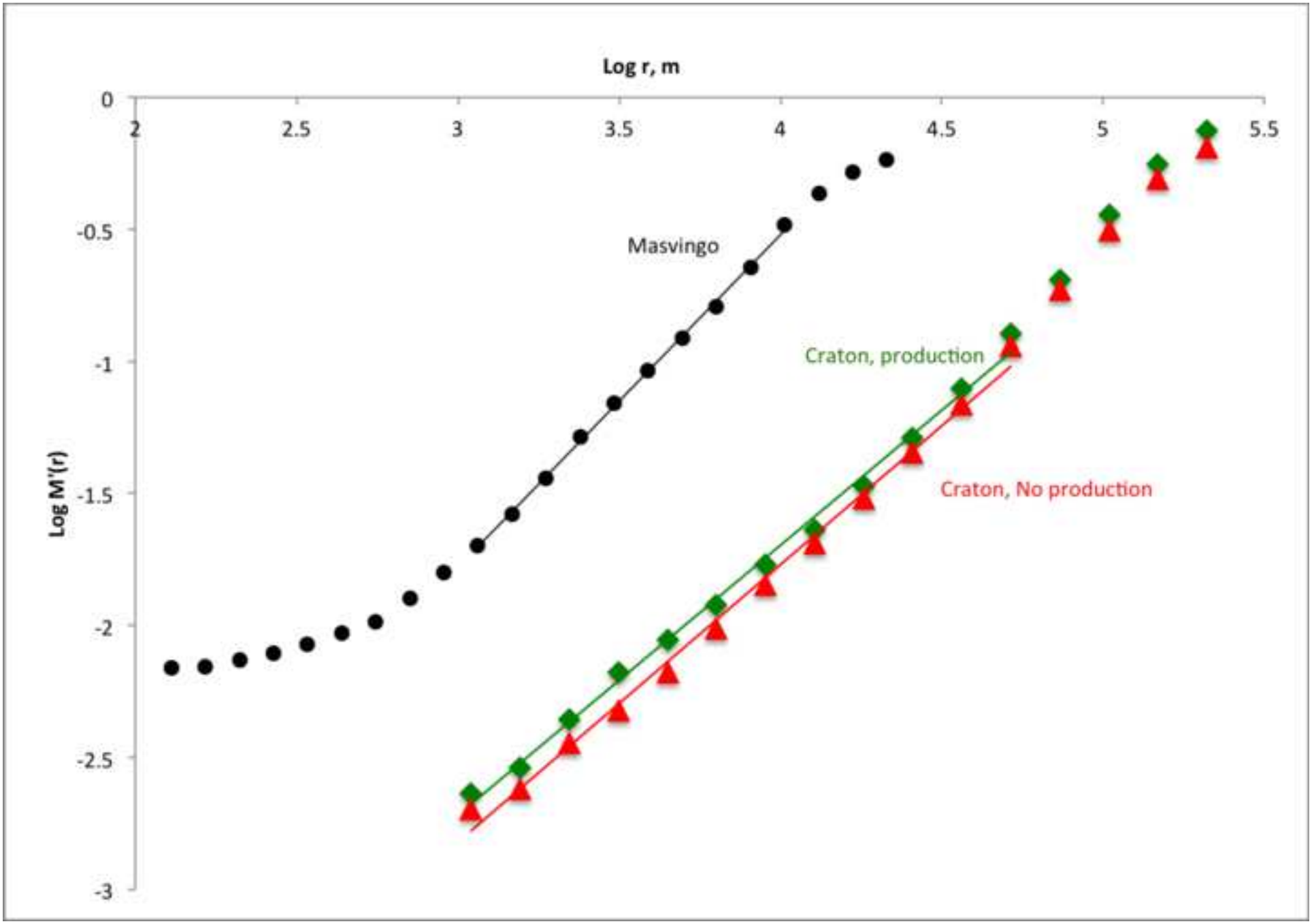

Figure8
Click here to download high resolution image

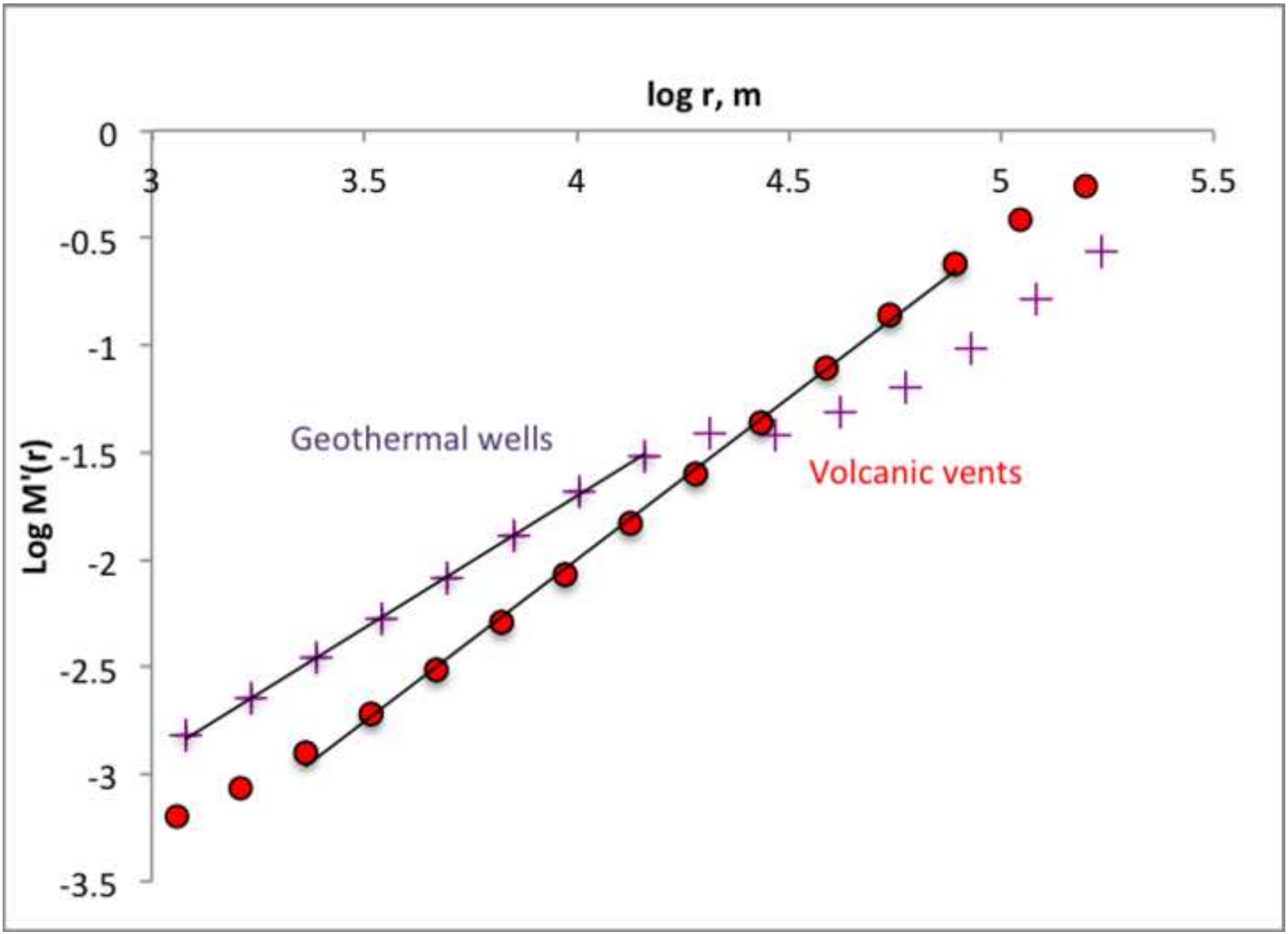

Figure9
Click here to download high resolution image

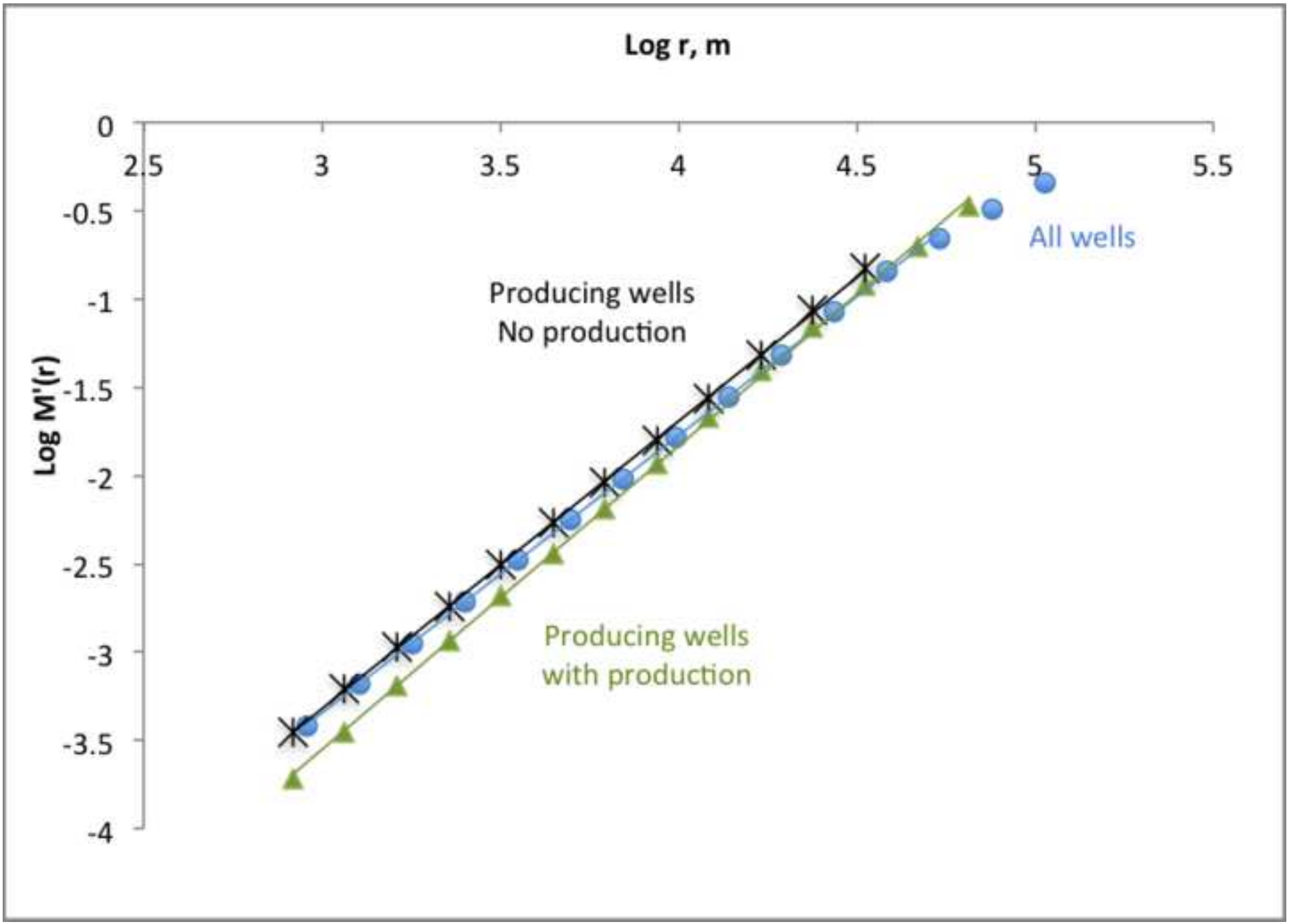

Figure10
Click here to download high resolution image

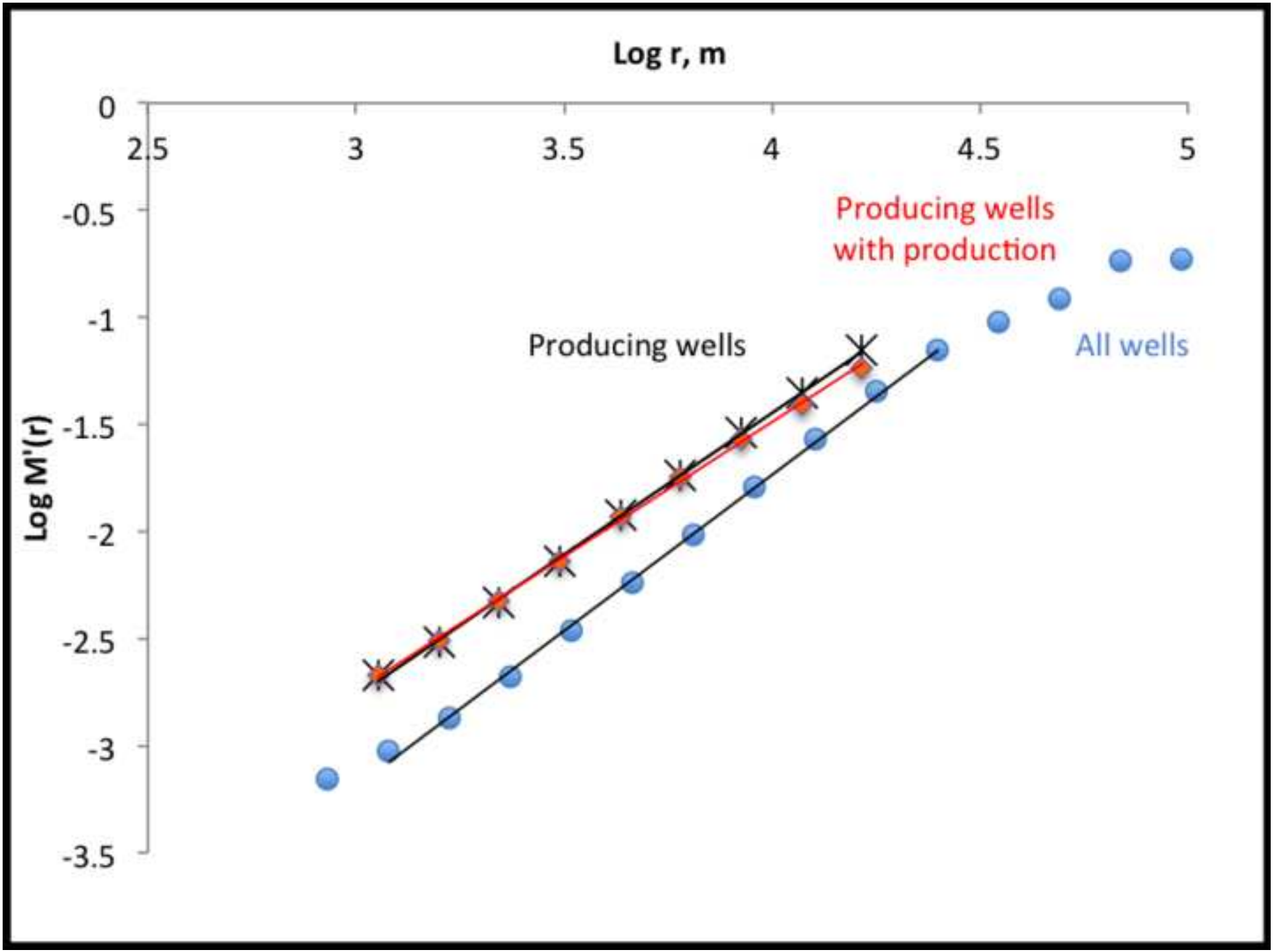

Table1
Click here to download Table: TABLE1.docx

Table 1. Data sources for this study. Mcf = million cubic feet. References:

1.Bartholomew 1991, 2. Wilson 1964; 1968, 3.

http://www.oregongeology.com/sub/gtilo/index.htm 4.

https://www.paoilandgasreporting.state.pa.us/publicreports/Modules/DataExports/DataExports.aspx

Commodity	Data	Location	N	Units	Source
Gold	Craton Mine Production	Zimbabwe	651	kg	1
Gold	Masvingo Mines	Zimbabwe	147		2
Geothermal Energy	Geothermal Wells	Oregon	5429		3
Volcanoes	Volcanic Vents	Oregon	2747		3
Gas	All Conventional Wells	Pennsylvania	62931		4
Gas	All Unconventional Wells	Pennsylvania	8686		4
Gas	Producing Conventional Wells	Pennsylvania	52856	Mcf	4
Gas	Producing Unconventional Wells	Pennsylvania	2878	Mcf	4

Table2
Click here to download Table: TABLE2.docx

Table 2. Mass dimensions (*Dm*) and mass-radius scaling exponents (*Dmr*) for data sets in this study. OR, PA: Oregon, Pennsylvania.

E = standard error of regression, R - Correlation coefficient, L, U – Lower and Upper limits of regression, k

Resource	**Gold**	**Geothermal**	**Gold**	**Unconvent Gas**	**Unconvent Gas**	**Geothermal**	**Convent Gas**	**Convent Gas**
Data	Craton prodn.	Wells	Mines	Prod. Wells	All Wells	VolcanicVents	All Wells	Prod. Wells
Region	Zimbabwe	OR	Masvingo	PA	PA	OR	PA	PA
Dm	1.05	1.23	1.25	1.26	1.45	1.51	1.57	1.63
E	0.022	0.009	0.014	0.012	0.017	0.017	0.006	0.005
R	0.997	1.000	0.999	1.000	0.999	0.999	1.000	1.000
L	1	12	9	11	1	23	1	1
U	52	144	103	16	25	779	54	33
Dmr	1.02			1.32				1.72
E	0.019			0.012				0.008
R	0.998			1.000				1.000
L	1			1				1
U	52			16				65

Table 3. Fractal Dimensions of 2 and 3D Bethe Lattices below, at and above the percolation threshold. *p* is the probability of a lattice node being occupied; *pc* is the probability at the percolation threshold (Stauffer and Aharony 1994).

	2D	**3D**
p<pc	1.56	2
p=pc	1.90	2.53
p>pc	2	3